

Production and Decays of W_R bosons at the LHC

Mariana Frank^a, Alper Hayreter^a, and Ismail Turan^b

^a*Department of Physics, Concordia University,*

7141 Sherbrooke St. West, Montreal, Quebec, CANADA H4B 1R6, and

^b*Ottawa-Carleton Institute of Physics, Carleton University,*

1125 Colonel By Drive Ottawa, Ontario, Canada, K1S 5B6.

(Dated: November 1, 2018)

Abstract

With the advent of the LHC, it is important to devise clear tests for Physics Beyond the Standard Model. Such physics could manifest itself in the form of new charged bosons, whose presence is most naturally occurring in left-right symmetric models (LRSM). We analyze the single W_R boson production in an asymmetric left-right model, where the left and right quark mixing matrices are not constrained to be equal. We investigate the cross sections as well as branching ratios of W_R bosons at the LHC, including constraints from low energy phenomenology. We then look for most likely signals in $pp \rightarrow W_R t \rightarrow t$ (*di-jet*) production. Including the background, we find that LHC could show significant signals for the new charged bosons. We compare our results throughout with the manifest left-right symmetric model and comment on similarities and differences.

Keywords: LHC phenomenology, Left Right Symmetry, New Gauge Bosons

I. INTRODUCTION

While the Standard Model (SM) has provided a compelling picture of low energy interactions, it has been plagued by theoretical inconsistencies. More recently, experimental deviations from the predictions of the model (such as signals of neutrino masses and mixing [1]) have given further justification to building model of Physics Beyond the Standard Model. Additionally, the experimental outlook on testing these scenarios looks very promising. LHC data is expected to provide ample material for analysis. When the data becomes available, it would be difficult to disentangle expectations for different models. The task of theorists is to provide viable scenarios for Physics Beyond the Standard Model *and* to predict the signals which distinguish them from the SM and from each other.

A large variety of models is available, all of which attempt to resolve some theoretical inconsistency of the SM. Of these, a particularly simple model is the Left Right Symmetric Model (LRSM) [2]. Originally introduced to resolve the parity and neutrino mass problems, it remains one of the simplest extensions of the SM, and it is a natural scenario for the seesaw mechanism [3]. The Higgs sector of the LRSM and its signals at accelerators have been thoroughly analyzed by theorists [4], and experimentalists have been particularly keen to search for doubly charged Higgs bosons, predicted in most versions of the model [5]. Less attention has been paid to the vector boson sector. The LRSM extends the gauge group of the SM to $SU(2)_L \times SU(2)_R \times U(1)_{B-L}$, and thus predicts the existence of two extra gauge bosons: a neutral Z_R and a charged W_R . While an extra neutral gauge boson Z' is predicted by several extensions of the SM, all containing an extra gauged $U(1)$ symmetry group, a charged gauge boson would be a more likely indication of left right symmetry¹.

Several other models predict the existence of extra W' bosons, such as extra dimensional models (both Randall Sundrum [6] and Universal Extra Dimensions model [7]), Little Higgs models [8] and Composite Higgs models [9]. The W' predicted in these models have features which distinguish them from LRSM, which we will discuss after our analysis.

Production of extra charged vector bosons at colliders has received less interest than that of Z' , although one study exists for the Tevatron [10]. However, recently, papers have appeared which analyze chiral couplings of a W' at LHC and indicate how to disentangle left or right handed bosons [11]. In the present work, we follow a different procedure. Assuming

¹ While the existence of W_R is present in several gauge unification scenarios, models with extra W_L bosons also exist.

the extra charged vector boson to come from a version of LRSM (and thus be right-handed), we analyze the production mechanism, decay rates and possible signals at the LHC.

W_R bosons are predicted to be heavy, of $\mathcal{O}(\text{TeV})$ and thus the signal expected to be much below the W_L production signal. But this is only the case if the quark mixing matrix in the right-handed sector (V_{CKM}^R) is either identical, or equal up to a diagonal matrix, to the one in the left-handed sector (the usual Cabibbo-Kobayashi-Maskawa V_{CKM}^L)—the so called *manifest* and *pseudo-manifest* LRSM, respectively. We describe the distinctive features of these models in the next section. This does not have to be the case, as was discussed at length by Langacker and Sankar [12], who allow right handed mixing matrices V_{CKM}^R with large off-diagonal elements. They perform a thorough investigation of the constraints on the mass of W_R and its mixing with W_L under these circumstances, and find out that the W_R mass can be a lot lighter, $M_{W_R} > 300 \text{ GeV}$ [13]. In what follows, we refer to this model and its variants as the asymmetric left-right model.

In the age of LHC, there is another immediate advantage of the asymmetric left-right model: such a W_R boson can be produced at rates larger by orders of magnitude than for models in which $V_{CKM}^R = V_{CKM}^{L*} K$, where K is a diagonal phase matrix. One could see this by looking at the signal $pp \rightarrow W_{L,R} t$. This single-top production cross section is known to be important in identifying and distinguishing between different new physics models, as these can have different effects (s -channel or t -channel) on the production process [14]. The partonic cross section at LHC is dominated by qg , with $q = d, s$. However for W_L production one must rely on the process $gb \rightarrow b \rightarrow tW$, and thus be disadvantaged by the small amount of b quarks in the proton; or rely on $gd(s) \rightarrow d(s) \rightarrow tW$, which is suppressed by the V_{ts}^L or V_{td}^L element of the V_{CKM}^L . However, if the off-diagonal V_{ts}^R or V_{td}^R elements of the V_{CKM}^R are large, one could produce W_R copiously. Additionally if there are less stringent restrictions on the W_R mass, one can envisage that W_R production could be observable, and if so, a clear distinguishing signal for LRSM. At the Tevatron, the production cross section is dominated at the partonic level by $q\bar{q}$, with $q = u, d, s, c$. Even for a light W_R boson, we would not expect any enhancements due to non-diagonal entries in the V_{CKM}^R , and the same is true for linear colliders.

The sensitivity of the Tevatron to W_R searches has been thoroughly discussed in [10]. Mass limits from the existing data depend on the ratio of the coupling constants for $SU(2)_R$ and $SU(2)_L$, g_R/g_L , on the nature and mass of the right-handed neutrinos ν_R , on the leptonic

branching ratio for W_R , on the form of the right-handed CKM matrix V_{CKM}^R . The most stringent experimental bounds from Tevatron searches are $M_{W_R} \geq 1$ TeV, under very specific assumptions (looking for W_R decays into an electron and a neutrino, for Standard Model-like couplings to fermions) [15]. As their assumptions would not apply for our model, we investigate the possible signals and mass bounds at the Tevatron in *dijet* production before proceeding with the LHC signal analysis.

The LHC thus presents a unique opportunity to observe such a W_R boson. We propose to investigate this possibility in the present paper. In a previous paper [16], we have laid the foundation of flavor-changing studies in left-right models by analyzing the most general restrictions on the parameter space of the model (M_{W_R} , M_{H^\pm} , V_{CKM}^R , and g_R/g_L) coming from $b \rightarrow s\gamma$, $B_d^0 - \bar{B}_d^0$ and $B_s^0 - \bar{B}_s^0$ mixings. For consistency, we include here these parameter space restrictions, as well as those coming from the Kaon physics.

We will proceed as follows. In Section II we will review the existing models and define the free parameters. We then briefly summarize the constraints on the W_R mass and mixing coming from K and B meson phenomenology in Section III. We then investigate the production and decays of W_R bosons at the LHC under different V_{CKM}^R parametrizations, and indicate which type can produce the most promising signals in Section IV. There we analyze the background and give an idea of the signals expected at LHC. We conclude and summarize our findings in Section VI.

II. LEFT-RIGHT SYMMETRIC MODELS

The idea of the original model was to construct a model based on $SU(2)_L \times SU(2)_R \times U(1)$ whose Lagrangian was invariant under a discrete left-right symmetry [2]. This implied that the gauge couplings g_L and g_R were equal and the Yukawa couplings were also restricted. Parity violation occurred through spontaneous symmetry breaking and provided different masses for W_L and W_R bosons².

Then the idea of discrete left-right (LR) symmetry was explored, where LR symmetry was assumed broken at a higher scale than the $SU(2)_L \times SU(2)_R \times U(1)$ breaking scale, which allows $g_L \neq g_R$. This led to *manifest LR symmetric models* [17], where the CP violation is

² These models run into difficulty because they predict $\sin^2 \theta_W$ too large and have problems with the baryon asymmetry and cosmological domain walls [12].

generated by complex Yukawa couplings, while the vevs of the Higgs fields remain real. This implies the same mixing for right and left-handed quarks, $V_{CKM}^R = V_{CKM}^L$, where V_{CKM}^L is the usual Cabibbo-Kobayashi-Maskawa matrix.

In *pseudo-manifest LR symmetry* both CP and P symmetries are spontaneously broken [18], such that the Yukawa couplings are real. In that case the left and right handed quark mixings are related through $V_{CKM}^R = V_{CKM}^{L*} K$, with K a diagonal phase matrix. Since in this model CP is spontaneously broken, this scenario shares the problems of the model invariant under discrete LR symmetry.

As problems seem to be consequences of requiring $V_{CKM}^L = V_{CKM}^R$, Langacker and Sankar have abandoned it in favor of a more general LR model [12] (which we call the asymmetric model, because mixings in the left and right handed quark sectors are not required to be the same, or related). The model was further analyzed in [19], with emphasis on CP violation properties.

We summarize the left-right model below without assuming either manifest or pseudo-manifest LR symmetry, and with no assumptions about coupling constants or neutrino masses. We allow a completely arbitrary right-handed quark mixing matrix V_{CKM}^R .

We assume a generic left-right symmetric model based on the gauge group $SU(3)_C \times SU(2)_L \times SU(2)_R \times U(1)_{B-L}$. The matter fields of this model consist of three families of quark and lepton fields with the following transformations under the gauge group:

$$\begin{aligned} Q_L^i &= \begin{pmatrix} u_L^i \\ d_L^i \end{pmatrix} \sim (3, 2, 1, 1/3), & Q_R^i &= \begin{pmatrix} u_R^i \\ d_R^i \end{pmatrix} \sim (3, 1, 2, 1/3), \\ L_L^i &= \begin{pmatrix} \nu_L^i \\ e_L^i \end{pmatrix} \sim (1, 2, 1, -1), & L_R^i &= \begin{pmatrix} \nu_R^i \\ e_R^i \end{pmatrix} \sim (1, 1, 2, -1), \end{aligned} \quad (2.1)$$

where the numbers in the brackets represent the quantum numbers under $(SU(3)_C, SU(2)_L, SU(2)_R, U(1)_{B-L})$. The Higgs sector consists of one bidoublet :

$$\Phi = \begin{pmatrix} \phi_1^0 & \phi_2^+ \\ \phi_1^- & \phi_2^0 \end{pmatrix} \sim (1, 2, 2, 0), \quad (2.2)$$

with vevs

$$\langle \Phi \rangle = \begin{pmatrix} k & 0 \\ 0 & k' \end{pmatrix}. \quad (2.3)$$

Additional Higgs multiplets are needed to break the symmetry to the SM and to generate a large mass of W_R compared to W_L . One can introduce doublets

$$\delta_L = \begin{pmatrix} \delta_L^+ \\ \delta_L^0 \end{pmatrix} \sim (0, 2, 0, 1), \quad \delta_R = \begin{pmatrix} \delta_R^+ \\ \delta_R^0 \end{pmatrix} \sim (0, 0, 2, 1) \quad (2.4)$$

with vevs $\langle \delta_{L,R}^0 \rangle = v_{\delta_{L,R}}$. If $v_{\delta_R} \gg (k, k', v_{\delta_L})$, this choice can generate a large mass for right-handed gauge boson (M_{W_R}) and a large right-handed Dirac neutrino mass. A popular alternative is to introduce Higgs triplets

$$\Delta_L = \begin{pmatrix} \frac{\Delta_L^+}{\sqrt{2}} & \Delta_L^{++} \\ \Delta_L^0 & -\frac{\Delta_L^+}{\sqrt{2}} \end{pmatrix} \sim (1, 3, 1, 2), \quad \Delta_R = \begin{pmatrix} \frac{\Delta_R^+}{\sqrt{2}} & \Delta_R^{++} \\ \Delta_R^0 & -\frac{\Delta_R^+}{\sqrt{2}} \end{pmatrix} \sim (1, 1, 3, 2). \quad (2.5)$$

The vev for right-handed triplet Higgs boson $\langle \Delta_R \rangle = v_{\Delta_R}$ can also produce a large M_{W_R} mass and generate a large Majorana neutrino mass.

Note that in general neither δ_L nor Δ_L Higgs bosons are required, unless one imposes left-right symmetry on the theory. v_{Δ_L} can generate a Majorana mass for the left handed neutrino, but must be very small (neutral current constraints). As we want to keep the model general, we keep both triplets and doublet representations.

The vector bosons of $SU(2)_R$, W_R^\pm and W_R^0 mix with the SM vectors in the charged and neutral sectors, respectively. Here we are interested in the charged boson sector, as observation of a W_R boson would be a clear signal for LR symmetry, so we present the masses and mixing for the charged states only. In general, W_L and W_R will mix to form mass eigenstates W_1 and W_2

$$\begin{aligned} W_L &= W_1 \cos \xi - W_2 \sin \xi \\ W_R &= e^{i\omega}(W_1 \sin \xi + W_2 \cos \xi) \end{aligned} \quad (2.6)$$

with ξ a mixing angle and ω a CP violating phase [20]. If ξ is small, then W_L and W_R approximately coincide with W_1 and W_2 . The mass matrix for the charged bosons will be

$$\begin{aligned} M_W^2 &= \begin{pmatrix} \frac{1}{2}g_L^2(|k|^2 + |k'|^2 + |v_L|^2) & -g_L g_R k' k^* \\ -g_L g_R k'^* k & \frac{1}{2}g_R^2(|k|^2 + |k'|^2 + |v_R|^2) \end{pmatrix} \\ &= \begin{pmatrix} M_L^2 & M_{LR}^2 e^{i\omega'} \\ M_{LR}^2 e^{-i\omega'} & M_R^2 \end{pmatrix} \end{aligned} \quad (2.7)$$

with $|v_{L,R}|^2 = |v_{\delta_{L,R}}|^2 + 4|v_{\Delta_{L,R}}|^2$ and $\omega' = \text{Arg}(k^*k')$. The mass eigenvalues are

$$M_{1,2}^2 = \frac{1}{2}\{M_L^2 + M_R^2 \mp [(M_R^2 - M_L^2)^2 + 4|M_{LR}^2|^2]^{1/2}\} \quad (2.8)$$

and the angles are

$$\tan 2\xi = \frac{\mp 2M_{LR}^2}{M_R^2 - M_L^2}, \quad e^{i\omega} = \pm e^{i\omega'} \quad (2.9)$$

where M_L and M_R are the mass parameters associated with $SU(2)_L$ and $SU(2)_R$ groups, respectively. For $|v_R| \gg (|k|^2, |k'|^2, |v_L|^2)$ the masses become approximately

$$\begin{aligned} M_1^2 &\simeq \frac{1}{2}g_L^2(|k|^2 + |k'|^2 + |v_L|^2), \\ M_2^2 &\simeq \frac{1}{2}g_R^2|v_R|^2 \end{aligned} \quad (2.10)$$

and

$$\xi \simeq \pm \frac{g_L}{g_R} \frac{2|kk'|}{|v_R|^2} \simeq \sin 2\beta \left(\frac{M_L}{M_R} \right) \quad (2.11)$$

where $\tan \beta = \frac{k}{k'}$.

The charged right-handed bosons contribute to the charged current for the quarks, which is

$$\mathcal{L} = \frac{g_L}{\sqrt{2}} \bar{u}_{iL} \gamma_\mu V_{CKM}^L{}_{ij} d_{jL} W_L^{\mu+} + \frac{g_R}{\sqrt{2}} \bar{u}_{iR} \gamma_\mu V_{CKM}^R{}_{ij} d_{jR} W_R^{\mu+} \quad (2.12)$$

and similarly for the leptons, which are allowed to mix with different CKM-type matrices.

We adopt the Wolfenstein parametrization for the CKM matrix V_{CKM}^L [13]

$$V_{CKM}^L = \begin{pmatrix} 1 - \frac{\lambda^2}{2} & \lambda & A\lambda^3(\rho - i\eta) \\ -\lambda & 1 - \frac{\lambda^2}{2} & a\lambda^2 \\ A\lambda^3(1 - \rho - i\eta) & -A\lambda^2 & 1 \end{pmatrix}. \quad (2.13)$$

For the right-handed CKM matrix we allow arbitrary mixing between the second and third generations, or between the first and third generations. To simplify the notation, we drop the CKM subscript and, following [12], denote the parametrizations as (A) and (B), where

$$V_{(A)}^R = \begin{pmatrix} 1 & 0 & 0 \\ 0 & \cos \alpha & \pm \sin \alpha \\ 0 & \sin \alpha & \mp \cos \alpha \end{pmatrix}, \quad V_{(B)}^R = \begin{pmatrix} 0 & 1 & 0 \\ \cos \alpha & 0 & \pm \sin \alpha \\ \sin \alpha & 0 & \mp \cos \alpha \end{pmatrix}, \quad (2.14)$$

with α an arbitrary angle ($-\pi/2 \leq \alpha \leq \pi/2$). In parametrization (A), depending on the values of α , the dominant coupling could be V_{ts}^R while in (B), the dominant coupling could

be V_{id}^R . These parametrizations are by no means the most general. The most general right-handed quark mixing matrix would be a CKM-type matrix, but with arbitrary entries. The (A) and (B) parametrizations are regions of the parameter space which allow relaxing the mass limit on W_R , and obeying the restrictions on Δm_K without fine-tuning.

The form of the CKM matrix in the right-handed quark sector affects low energy phenomenology, in particular processes with flavor violation, and thus restricts the mass M_{W_R} and mixing angle ξ . Several studies for W_R production [21] and mass constraints [22] exist in the literature, but most of them are based on either the manifest, or the pseudo-manifest LRSM. We calculate the production cross section and decays of the W_R bosons in the LRSM with large off-diagonal entries in the V_{CKM}^R matrix, and express the results as functions of these parameters, and include constraints from both Kaon and B meson sectors. We confine ourselves to a general version of the model and make no specific assumptions about the nature and mass of the neutrinos. We summarize these constraints in the next section.

III. CONSTRAINTS ON LEFT-RIGHT SYMMETRIC MODELS FROM LOW ENERGY PHENOMENOLOGY

Before proceeding with the evaluation of the W_R production and decays, we summarize briefly the constraints on the parameter space of the left-right model, mostly from flavor violating processes, which are relevant to the study of W_R phenomenology.

A. $K^0 - \bar{K}^0$ mixing

Restrictions coming from Kaon physics have been analyzed by several authors. For the pseudo-manifest left-right symmetric model, evaluation of ΔM_K and ϵ_K restricts the right-handed charged boson mass, $M_{W_R} > 1.8$ TeV [23], while in more recent analyses of the model, where parity or charge conjugation is chosen to be broken spontaneously, $M_{W_R} > 2.5$ TeV [24]. In the Langacker and Sankar parametrization, which we study here, the limit is much lower $M_2 \geq 300 \frac{g_R}{g_L}, 340 \frac{g_R}{g_L}, 670 \frac{g_R}{g_L}, 350 \frac{g_R}{g_L}$ GeV, respectively for the four parametrizations ($V_{(A)}^R, V_{(B)}^R$, with both \pm signs in the right CKM elements) [12].

B. $B_d^0 - \bar{B}_d^0$ and $B_s^0 - \bar{B}_s^0$ mixing

For the pseudo-manifest left-right model the $W_R - W_L$ box diagram does not have an important effect. However, for Langacker parametrization $U_{(B)}^R$ the limit is $M_2 \geq 1384 \frac{g_R}{g_L}$ GeV [25]. The most comprehensive analysis of the constraints coming from B meson mixing and decays in the Langacker parametrization is presented in [26]. For more up-to-date constraints, including the recent data, see [16].

C. $b \rightarrow s\gamma$

Previous studies in left-right models originate from [27], while other constraints are presented in [28]. The constraints on $b \rightarrow s\gamma$ were thoroughly analyzed within the asymmetric model studied here, as well as in the manifest model in [16]. There are less restrictive than those coming from $B_d^0 - \bar{B}_d^0$ mixing, but complementary to $B_s^0 - \bar{B}_s^0$. These constraints depend on several parameters and are difficult to summarize; however, they are included in the cross section plots.

IV. PRODUCTION AND DECAYS

In this section we investigate the single production cross section at LHC of a W_R^\pm boson, $pp \rightarrow tW_R$, and decay branching ratios of the right-handed W boson in the scenarios in which the right-handed CKM matrix is $V_{(A)}^R$ (called U_A for simplicity), $V_{(B)}^R$ (called U_B for simplicity), as in (2.14), and compare the results to those obtained in the manifest left-right symmetric model (MLRSM). In the MLRSM, the CKM matrices in the left- and right-handed quark sectors are the same, and so are the coupling constants for $SU(2)_L$ and $SU(2)_R$. The only unknown parameter is the W_R mass; while in U_A and U_B the production and decay rates are also functions of $\sin \alpha$, the right-handed CKM parameter, as well as the ratio g_R/g_L of $SU(2)_L$ and $SU(2)_R$ coupling constants. The dominant partonic level Feynman diagrams are shown in Figure 1. The index i indicates that we sum over the three generations.

In Figure 2, top row we present the single W_R production cross section as a function of the W_R mass (in the 400-2000 GeV range) for three values of $\sin \alpha$. The three panels correspond to three values allowed for g_R/g_L : 0.6, 0.8 and 1. When $\sin \alpha$ is large, the

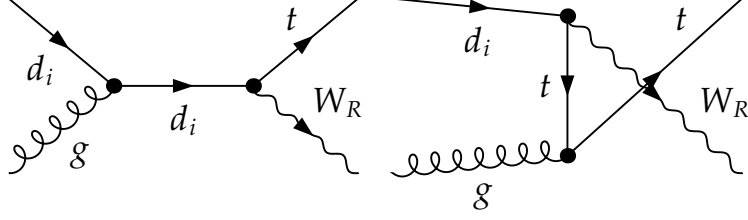


FIG. 1. The W_R -top associated production at the LHC

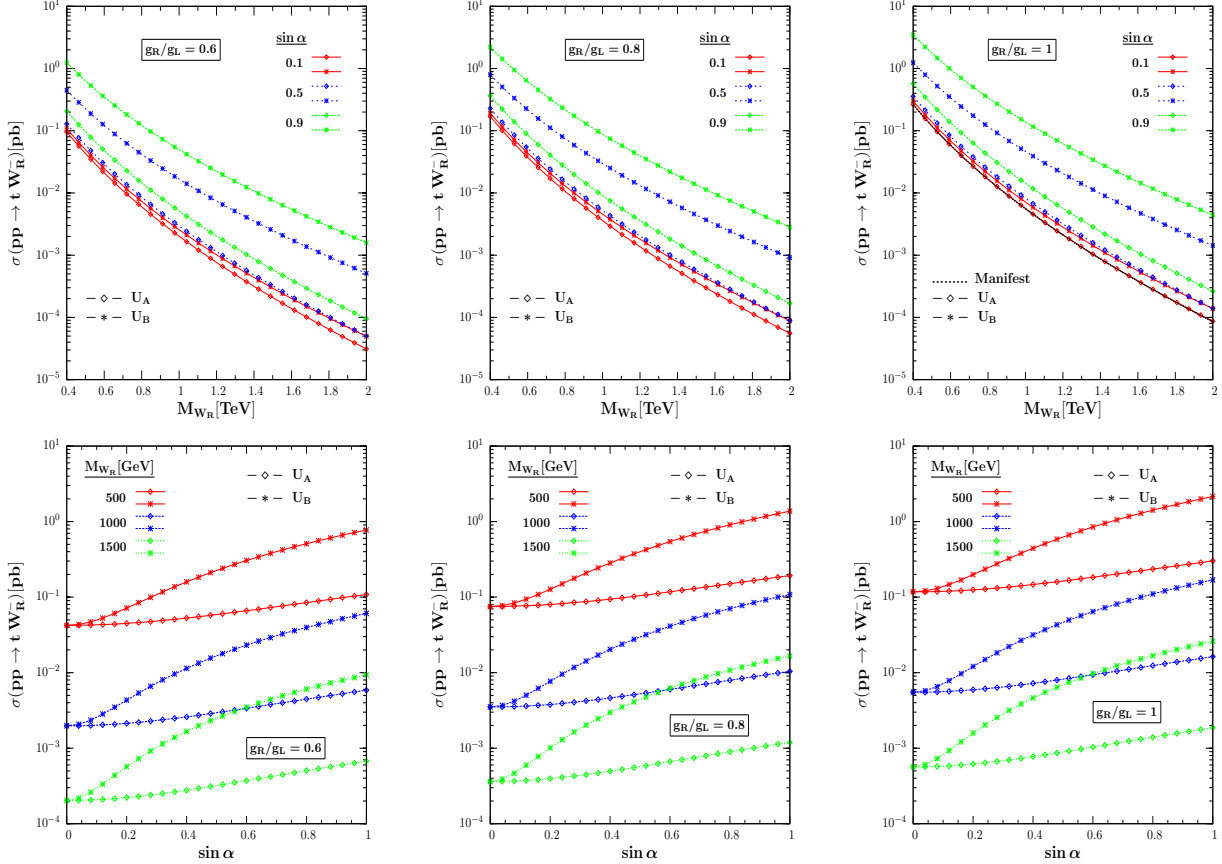


FIG. 2. W_R production cross-section as a function of W_R mass (upper panels) and right-handed CKM matrix parameter $\sin \alpha$ (lower panels), for the three models described in the text (U_A , U_B and manifest left-right symmetric model).

off diagonal CKM mixing element V_{td}^R or V_{ts}^R becomes large. As there are more d and s quarks than b in the proton, this enhances the hadronic contribution to the cross section for U_A and U_B cases. The production cross section decreases when W_R mass increases, or $\sin \alpha$ decreases. Similarly, the production cross section is enhanced by larger g_R/g_L . The MLRSM cross section overlaps with that of model U_A in the case of $\sin \alpha = 0.1$ (the right panel in the top row).

In the bottom row of Figure 2, we explore the dependence of the cross section in U_A and U_B on $\sin \alpha$ for three values of M_{W_R} . The three panels again represent cross sections for $g_R/g_L = 0.6, 0.8$ and 1 . Figure 2 shows that in the region of large $\sin \alpha$ and low M_{W_R} we can expect large enhancements in the production cross section. For suitable choices of $\sin \alpha$ and M_{W_R} (light W_R mass and large $\sin \alpha$ region), the cross section can reach 1 pb or more. The slight difference between U_A and U_B cross sections is attributed to the relative abundance of d over s quarks in the proton.

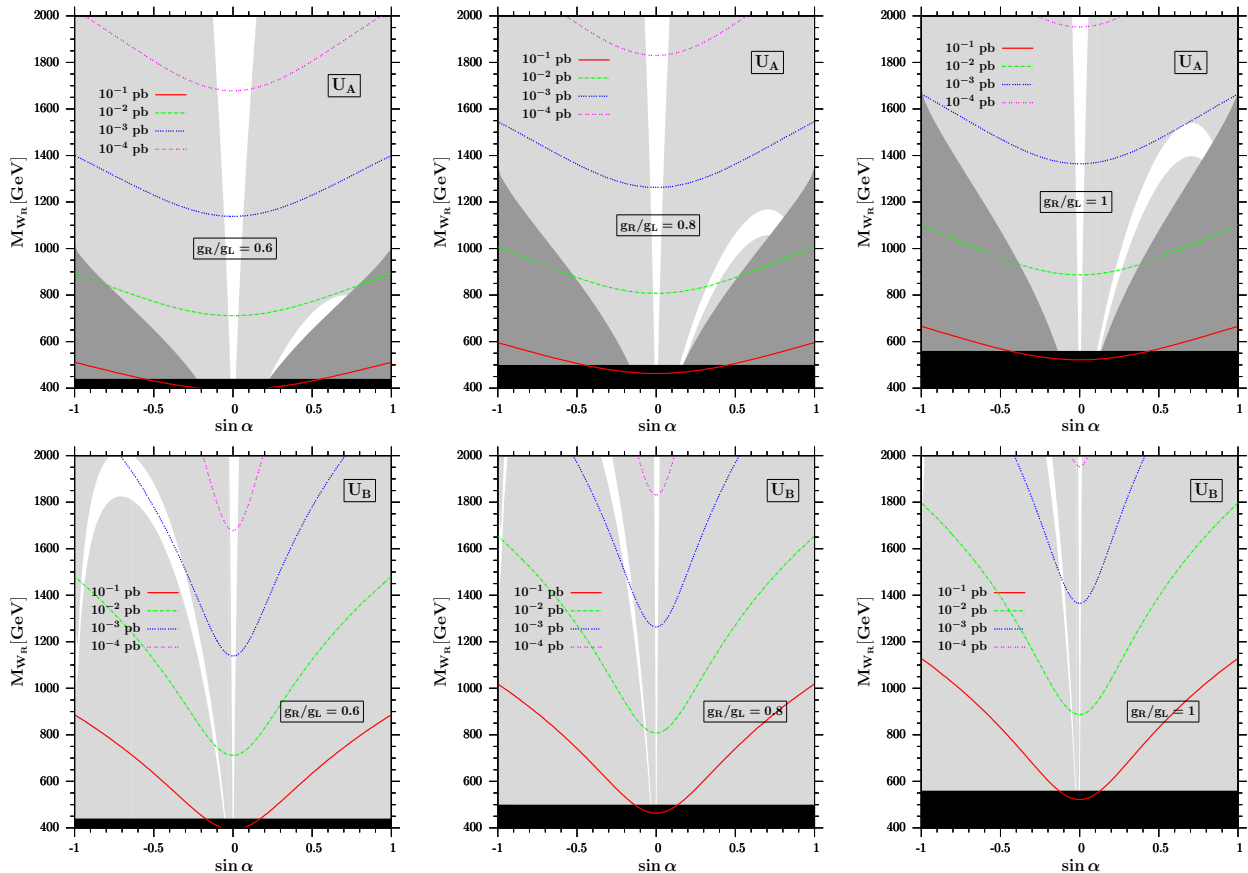


FIG. 3. Contour plot of (M_{W_R} vs $\sin \alpha$). Upper row is for U_A parametrization in which the W_R production cross-sections are constrained by both $b \rightarrow s\gamma$ and $B_s^0 - \bar{B}_s^0$ processes. Yellow shaded regions are excluded from $b \rightarrow s\gamma$ and dashed shaded regions from $B_s^0 - \bar{B}_s^0$. And dark shaded region indicates the exclusion by L-R mixing angle violation ($\xi < 3 \times 10^{-3}$). Lower row is for U_B parametrization where only $B_d^0 - \bar{B}_d^0$ mixing constrains the production cross-section. In both parametrizations we take $M_{H^+} = 20$ TeV and $\tan \beta = 30$.

In Figure 3, we give a contour plot in the $M_{W_R} - \sin \alpha$ parameter space, including constraints from $b \rightarrow s\gamma$, $B_d^0 - \bar{B}_d^0$, and $B_s^0 - \bar{B}_s^0$ processes. This plot correlates restrictions

on $\sin \alpha$, M_{W_R} , g_R/g_L and production cross sections. In the top row, we show the plot for the U_A parametrization. This parametrization is constrained by $b \rightarrow s\gamma$ branching ratio (in yellow) and $B_s^0 - \bar{B}_s^0$ mixing (dashed). The three panels represent increasing values of coupling constants ratio $g_R/g_L = 0.6, 0.8$ and 1 . The dark shaded parameter region at the bottom (increasing with larger g_R/g_L) represents restrictions due to the $W_L - W_R$ mixing angle $\xi < 3 \times 10^{-3}$. The most stringent phenomenological inputs which restrict the $W_L - W_R$ mixing angle ξ are: weak universality for light neutrinos, partial conservation of axial-vector-current in $K \rightarrow 2\pi$ and $K \rightarrow 3\pi$ and constraints on W_L mass, which is reduced by increasing ξ [12]. The parameter space is overall very restricted. For smaller g_R/g_L there is a stable allowed region around $\sin \alpha = 0$, which is decreasing with increasing g_R/g_L . However, for all coupling ratios, there is a parameter space allowed, where $\sin \alpha$ is large and positive, and the W_R mass can be relatively light ($M_{W_R} = 600 - 700$ GeV for $g_R/g_L = 0.6$) or intermediate ($M_{W_R} = 1400 - 1500$ GeV for $g_R/g_L = 1$). For these cases the cross section can be of order 10^{-2} pb.

The bottom row of Figure 3 presents the same restrictions on the $M_{W_R} - \sin \alpha$ parameter space in the U_B parametrization. The three panels again represent restrictions for $g_R/g_L = 0.6, 0.8$ and 1 . The restrictions come from $B_d^0 - \bar{B}_d^0$ (shaded) and the $W_L - W_R$ mixing angle $\xi < 3 \times 10^{-3}$ (dark shaded—this constraint is the same as in the upper row). The U_B parametrization is much more restricted, reflecting the stringent restrictions from $B_d^0 - \bar{B}_d^0$ mixing. While the same region around $\sin \alpha = 0$ exists in all graphs, it is shrunken very close to zero, especially for $g_R/g_L = 1$. The region for $\sin \alpha$ away from zero (in this case negative) is significant only for $g_R/g_L = 0.6$ and larger values of the W_R mass. Still, there is a small parameter space available for $M_{W_R} = 1.8 - 2$ TeV. But the cross section expected in this region is of order of 10^{-3} pb, smaller by a factor of 10 than that for the U_A parametrization.

In Figure 4 we present the branching ratios of W_R decays into quarks, and a representative one into $W_L h^0$ (assuming this decay has the phase space required to proceed) in the asymmetric left-right model. In the top panels, we analyze the decay width into quarks, as a function of $\sin \alpha$, for both U_A and U_B scenarios. The left panel corresponds to $M_{W_R} = 750$ GeV, the right one to $M_{W_R} = 1.5$ TeV. It is possible to include both parametrizations in one plot because, between these two scenarios, the CKM matrix elements involving s and d quarks mixing with t quarks are switched, and although the masses of these quarks are not identical, it does not significantly impact on the branching ratios. While $W_R^- \rightarrow d(s)\bar{u}$ is the

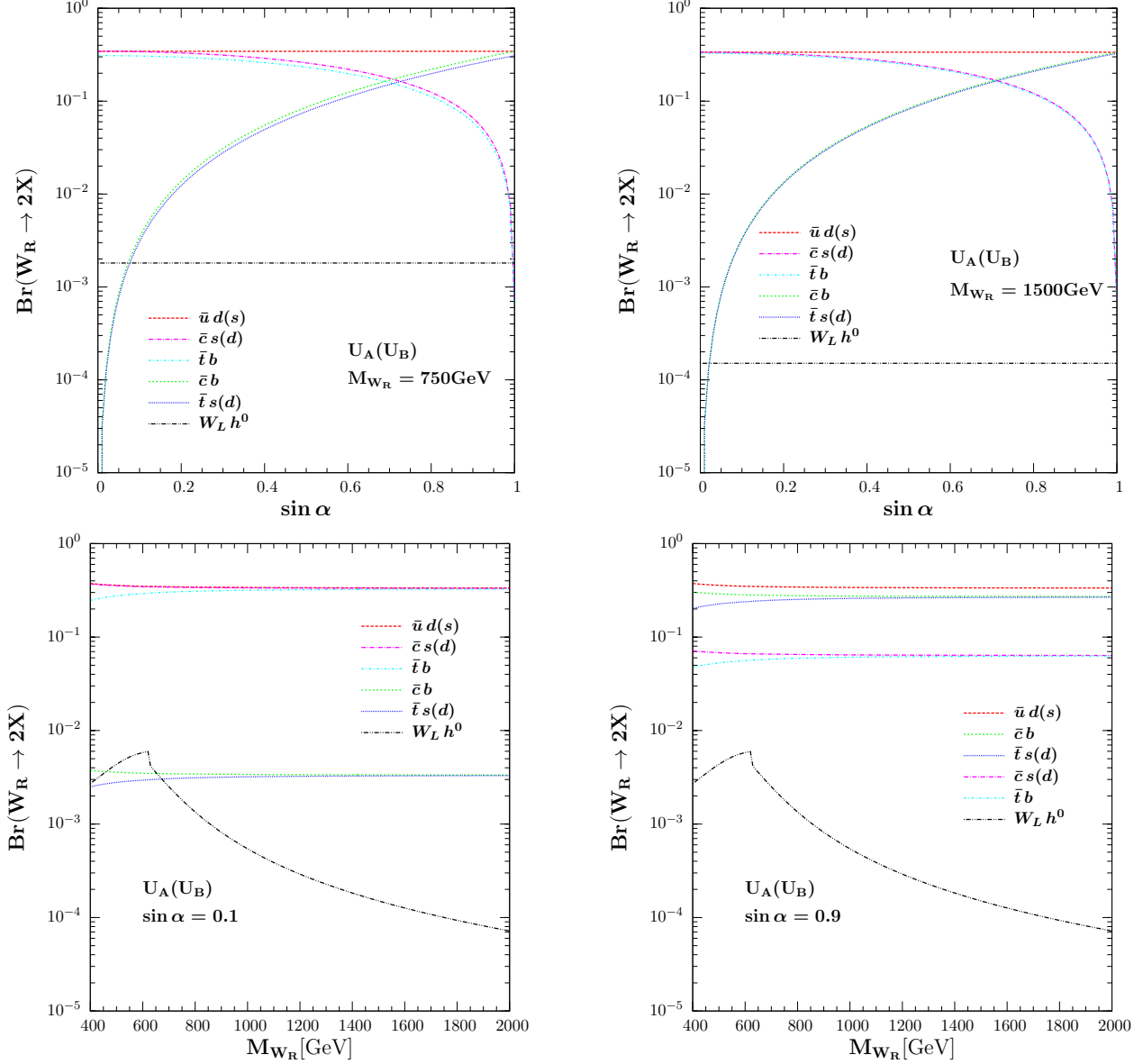


FIG. 4. Branching ratios of W_R decays as functions of $\sin \alpha$ (above panel) and W_R mass (below panels). The W_R mass is fixed at 750 GeV in left top and 1500 GeV in right top panel, while $\sin \alpha$ is fixed to 0.1 in left bottom panel and 0.9 in right one.

dominant decay for both cases, for large $\sin \alpha$ the branching ratios to $b\bar{c}$ and $d(s)\bar{t}$ become comparable; while for low $\sin \alpha$ the branching ratios to the same-generation pairs, $b\bar{t}$ and $s\bar{c}$, are large. The leptonic decays $W_R^- \rightarrow l^- \bar{\nu}_R$, ($l = e, \mu$) are not presented here, as we wanted to avoid extra assumptions on the nature of the neutrinos and their masses. Many other decay channels are possible, but we have chosen to only illustrate $W_L h^0$. It is possible that, for a range of the parameters, there is sufficient phase space for other decays (to leptons,

$h^0 H^\pm, Z_L H^\pm, \dots$) to proceed, but all require further assumptions. In our analysis, charged Higgs and all other neutral Higgs bosons except for h^0 are heavy, so these channels are not open. The branching ratio to $W_L h^0$ is independent of $\sin \alpha$ and always dominated by branching ratios to quarks.

The panels in the bottom row show the dependence on the same branching ratios as a function of M_{W_R} , for $\sin \alpha = 0.1$ (left panel) and $\sin \alpha = 0.9$ (right panel). The dominance of the $d(s)\bar{u}$ decay mode persists, and is independent of $\sin \alpha$, a consequence of the form chosen for V_{CKM}^R to agree with Kaon phenomenology. The branching ratios are independent of the mass of the W_R , with the exception of $W_L h^0$. Note that the branching ratios also do not depend on the coupling constant for $SU(2)_R$ (or g_R/g_L), as it appears as an overall factor in both the partial decay width and total width formulae.

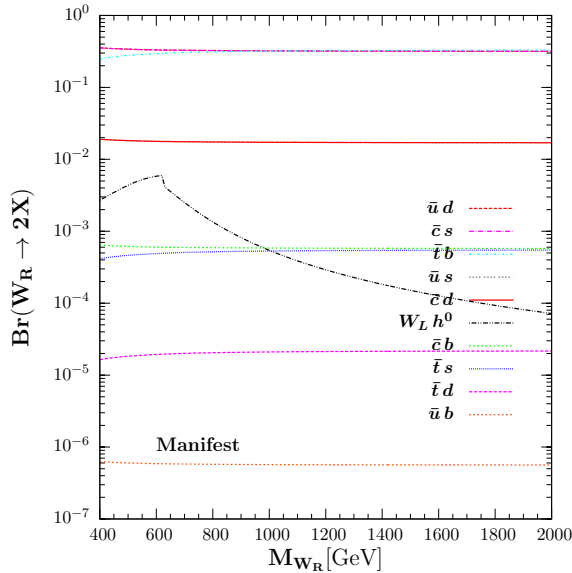


FIG. 5. Branching ratios of W_R decays as functions of W_R mass in Manifest Left-Right Model.

Figure 5 illustrates the branching ratios of all decay modes of the W_R boson in the MLRSM. The main difference from the point of view of observability is that in scenarios U_A, U_B there are 5 $q\bar{q}'$ decay modes with branching ratios between $5 \times 10^{-2} - 2 \times 10^{-1}$, while in MLRSM there are only 3 (for $M_{W_R} > 500$ GeV). In both cases, all the other branching ratios are much smaller and very similar in all three scenarios. For the purpose of explicit branching ratio calculations, we considered the case in which the bi-doublet Higgs boson is supplemented by triplet Higgs bosons. Under this assumption we diagonalized the Higgs mass matrix and calculated the Feynman rules. We expect the case with doublet Higgs

bosons to yield very similar results when we impose experimental constraints.

V. SIGNAL AND BACKGROUND FOR W_R PRODUCTION AT THE LHC

Before proceeding with the analysis of the W_R production signal at the LHC, we consider the signal at the Tevatron, from $p\bar{p} \rightarrow W_R \rightarrow dijet$. The *dijet* data is already available from CDF Run II [29], and the analysis shows no significant evidence for a narrow resonance. This is used to put mass constraints on several beyond the SM particles, including the W' . To compare the data with our model, we used CALCHEP software [30] and implemented the model into the software. To obtain the *dijet* spectrum we used the following detector cuts at $\sqrt{s} = 1.96$ TeV: $p_T > 40$ GeV, $|y| < 1$, $|\eta| < 3.6$ and $R_{\text{cone}} = 0.7$ (jet cone angle). The parameters used to generate Figure 6 are $M_{W_R} = 750$ GeV, $g_R/g_L = 1$, $\sin \alpha = 0.2(-0.05)$ for $U_A(U_B)$. The *dijet* process is dominated by s -channel contributions. From the figure we see that under these conditions, the W_R signal falls below the CDF data and would not be observable at the Tevatron. Thus we cannot expect to extract meaningful mass bounds for W_R , even for a relatively light gauge boson.

We then proceed with the investigation of the W_R production signal at the LHC. We simply considered a single *top* production associated with a *dijet* through a W_R exchange in both s - and t -channel processes as in Figure 6. Assuming b -jets are tagged and further *top* decays are reconstructed, we selected only light quarks (u, c, d and s) in jets. In order to compare our signal with the background we accounted all the possible *top* + *dijet* processes in the SM final state. For the signal analysis we used again the implementation of our model into the CALCHEP software [30]. We also introduced some basic detector cuts on the pseudorapidity ($|\eta| < 2$) and on the transverse energy ($p_T > 30\text{GeV}$). We assume that in both our model and in the SM, the top quark will decay as predicted, and it can be reconstituted. We have chosen W_R decays to quarks, rather than leptons, because we wanted to avoid assumptions on the nature and masses of neutrinos. Also, jets can be easily identified and this decay mode does not involve any missing energy, making it easier to detect a W_R resonance. We also restricted the decay products to jets (light quarks only) to avoid $t\bar{t}$ production. In the case of considering $W_R \rightarrow \bar{t}d_i$, the SM background would be $t\bar{t}j$ and could be significant.

In Figure 7 and Figure 8, we present W_R production signal at 14 TeV with different CKM

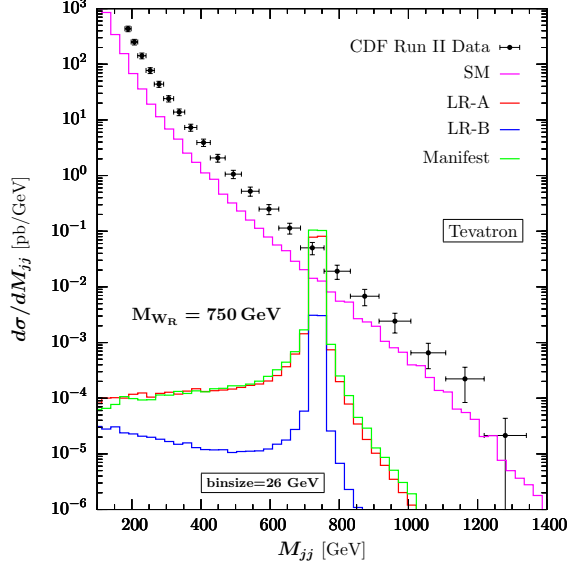


FIG. 6. Differential cross section for the *dijet* mass spectrum for W_R decays in the U_A , U_B parametrizations and in the Manifest Left-Right Model, compared to the SM background and the CDF data. It is possible to show that the SM curve fits very well with the CDF Run II data after including NLO perturbative QCD corrections. Our SM curve should be taken as a rough estimation.

parametrizations and compare it with the SM background. We choose the binsize to be 20 GeV, and plot the differential cross section with respect to the invariant *dijet* mass M_{jj} . It is clear that for all the parametrizations, the W_R signal can be observed as a resonance in the *dijet* invariant mass distribution at the LHC and is quite distinguishable from the SM background. The diagrams for the SM background are very similar to the ones in Fig. 6, W_R replaced with W_L as well as some other exchange diagrams. Signatures in U_A and U_B parametrizations are in the left and right columns of Figure 7. In first two rows we kept W_R

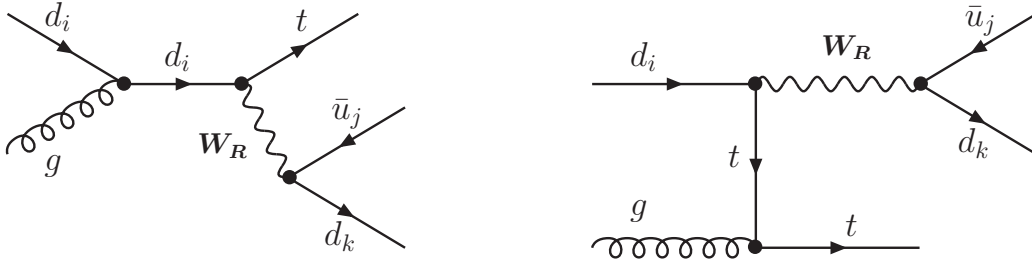


FIG. 7. The signal $pp \rightarrow t W_R \rightarrow t(\text{jet jet})$

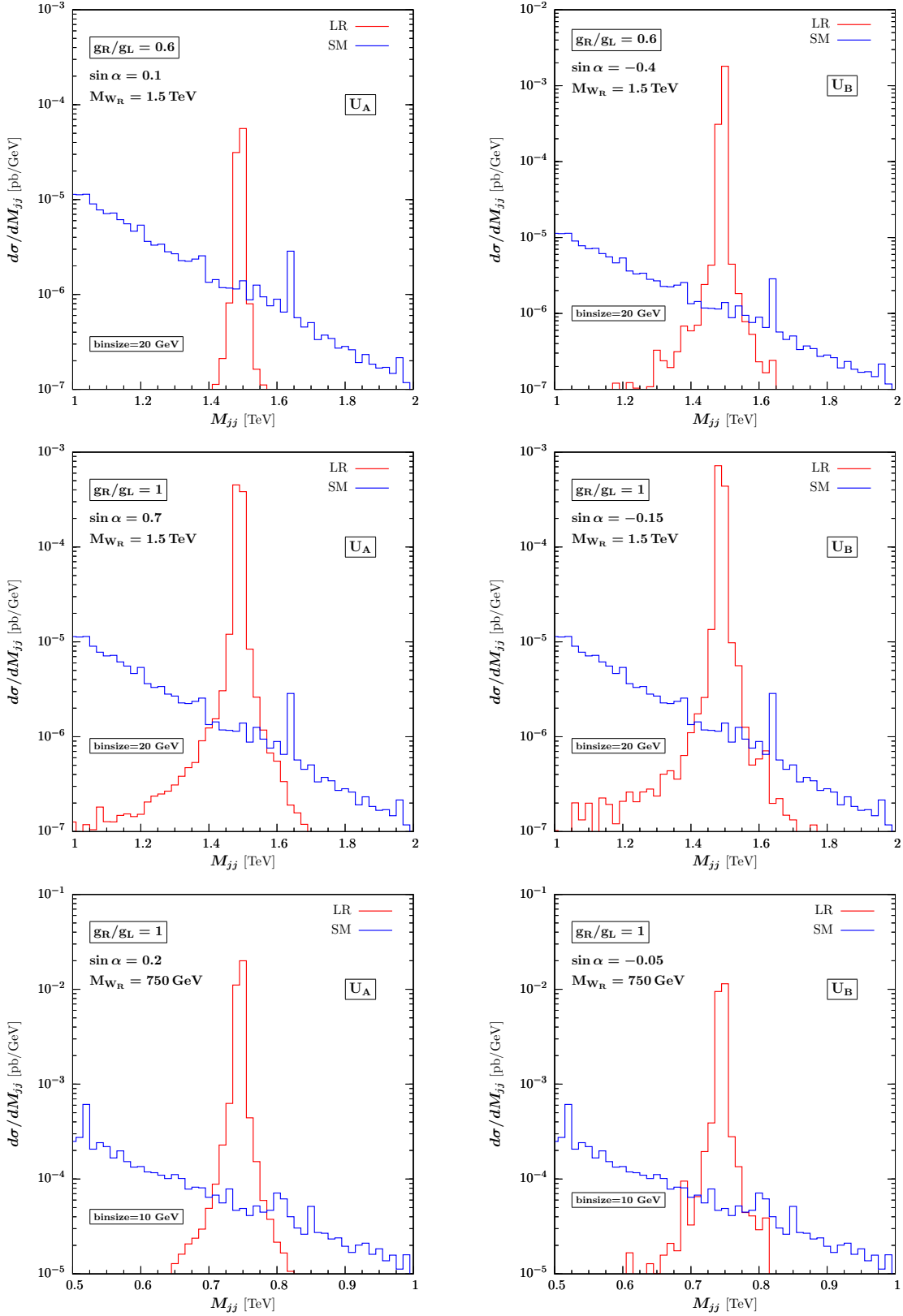


FIG. 8. W_R signal as a resonance in dijet mass distribution at the LHC with U_A (left column) and U_B (right column) right CKM parametrizations. The signal is observed in $p, p \rightarrow t, dijet$ process where only the light quarks are counted as jets. We choose $binsize = 20$ GeV for intermediate $M_{W_R} = 1500$ GeV and $binsize = 10$ GeV for light $M_{W_R} = 750$ GeV. The center of mass energy is 14 TeV.

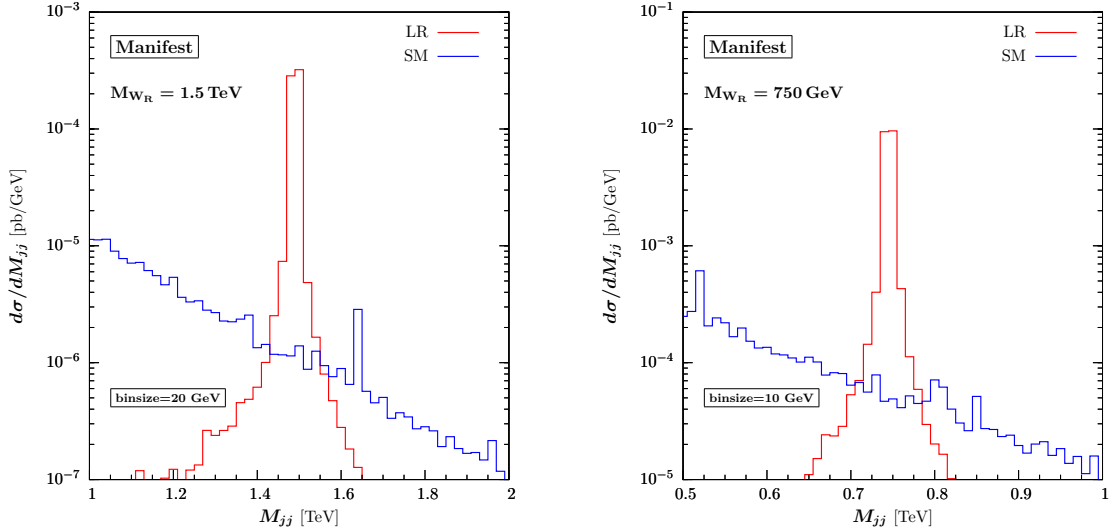


FIG. 9. The resonance W_R signal in the LHC with Manifest model. The intermediate W_R (on left panel) and light W_R (on right panel) signals are presented. Again the same *binsize* choice with Fig.7. The center of mass energy is 14 TeV.

mass at an intermediate value ($M_{W_R} = 1.5$ TeV) and changed the ratio of gauge coupling constants (g_R/g_L) as well as the right CKM matrix element ($\sin \alpha$) between the panels. The numerical values of these parameters are chosen according to the constraints from low energy phenomenology in Figure 3. In the last row we showed the signal of a lighter W_R ($M_{W_R} = 750$ GeV) with *binsize*= 10 GeV and equal gauge coupling constants ($g_R = g_L$) in the region allowed by the constraints. By comparison, in Figure 8 we show signatures for the W_R production and decay to *dijets* in the MLRSM model for the intermediate (left panel) and the light (right panel) W_R (the last for comparison only, as light W_R masses are largely excluded by Kaon phenomenology in the absence of extreme fine tuning). It is inferred from these figures that a new right handed charged gauge boson signal of left-right symmetry is very clear, distinct and accessible within the LHC's discovery limits. For a luminosity of 100 fb^{-1} at 14 TeV and a light W_R boson (both very optimistic assumptions), the signal can reach 100 events per year.

Whatever the model is, the cross-sections are robust, that is they are roughly the same order of magnitude, independent of the model used. The reason is the following : in U_A and U_B models there are fewer diagrams contributing to the differential cross sections, but the flavor violation from the right-handed quarks is stronger, whereas in the manifest left-right symmetric model there are more Feynman diagrams contributing to the differential cross section, but the flavor violating interactions in the right-handed sector are weaker. This

explains the resemblance of the signals between $U_A(U_B)$ and the MLRSM. To distinguish among the left-right models and to finely pinpoint the origin of the signal requires further detailed analysis with more realistic detector simulations.

VI. CONCLUSIONS

We analyzed the single production, decay and collider signals of W_R bosons produced in left-right symmetric models. We considered models with a general right-handed quark mixing structure (which we call the asymmetric left-right model), but constrained by the Kaon and B-meson flavor physics. We also compared the results with those of the manifest left-right symmetric model, where $V_{CKM}^R = V_{CKM}^L$ and the coupling constants in the left and right sectors are equal. In the asymmetric left right model, there is only one free parameter in the right-handed CKM mixing matrix. Additionally, the charged Higgs and W_R masses, as well as the ratio of the $SU(2)_L$ and $SU(2)_R$ coupling constants, are also free parameters. We included restrictions on the same parameter space coming from $B_{d,s}^0 - \bar{B}_{d,s}^0$ mixing and the branching ratio for $b \rightarrow s\gamma$ [16].

The dominant production mode is in association with a top quark, and this has a large background from the single top production (in association with W_L) from the standard model. However looking at events in the 500-2000 GeV mass range for W_R , we show that the SM background is always below the W_R background, and we expect a significant peak above the SM background around the W_R mass (assumed to be in the range considered). Even with a luminosity of 10 fb^{-1} , achievable at the LHC within the next 3 years, we expect several events a year, while with $\mathcal{L} = 100 \text{ fb}^{-1}$, the events could reach 100 per year. We concentrate our analysis in the $W_R \rightarrow dijet$ decay mode, where *dijets* are the light quarks u, d, s and c .

The cross section for the single W_R production can reach 10 fb, including all parameter restrictions, and the dominant decay modes are to light quarks, $\bar{u}d(s)$ being favored by the choice of parametrization, and $\bar{c}s(d)$ and $\bar{t}b$ by the restrictions on the right handed CKM.

Models which predict extra W' bosons all have features that distinguish them from W_R bosons in LRSM. In warped extra-dimensional models [6], the coupling of the extra charged gauge bosons to light quarks and leptons is suppressed relative to those in SM. By contrast, in LRM, the decays to leptons might be suppressed for heavy right-handed neutrinos, whereas

$W \rightarrow jet\ jet$ has no missing energy so the signal can be reconstructed in full. The irreducible SM background from the electroweak process (single top production) is shown to be smaller than the signal inside the resonance region. Warped RS models need luminosities of $\mathcal{L} = 100$ (1000) fb^{-1} for a W' to reach a statistically significant signal, and expected W' masses are in the 2-3 TeV region. Technicolor or composite Higgs [9] models are expected to give very similar signals, as the warped extra dimensional model is dual to the 4D strong dynamics involved in electroweak symmetry breaking. In the Little Higgs Models [8], the heavy W_H is left-handed and the partial width to each fermion species is almost the same (for massless fermions). In UED, the additional (KK) W and Z bosons expected to have masses in the 100-200 GeV region [7], have their hadronic decays closed, so they decay democratically to all lepton (one KK and one ordinary) flavors.

A clear signal for a charged vector boson will be much more significant than one for a neutral Z' boson, as it would restrict the extension of the gauge sector. Our analysis is complementary to previous analyses which indicate how to find whether the extra charged W' boson is left or right-handed, by presenting the signals expected for W_R in LRM, both manifest (with $V_{CKM}^R = V_{CKM}^L$) and in a case where V_{CKM}^R , constrained by B and K phenomenology, is independent on the mixing in the left-handed quark sector and characterized by a single parameter. The signal for such a charged gauge boson is significantly different than in other scenarios with extra W' s and would be an irrefutable signal of left-right symmetry.

-
- [1] Y. Fukuda *et al.* [Super-Kamiokande Collaboration], Phys. Rev. Lett. **81**, 1562 (1998).
 - [2] J. C. Pati and A. Salam, Phys. Rev. D **10**, 275 (1974) [Erratum-ibid. D **11**, 703 (1975)]; R. N. Mohapatra and J. C. Pati, Phys. Rev. D **11**, 566 (1975); R. N. Mohapatra and J. C. Pati, Phys. Rev. D **11**, 2558 (1975); G. Senjanovic and R. N. Mohapatra, Phys. Rev. D **12**, 1502 (1975); R. N. Mohapatra, F. E. Paige and D. P. Sidhu, "Symmetry Breaking And Naturalness Of Parity Conservation In Weak Neutral Phys. Rev. D **17**, 2462 (1978); G. Senjanovic, Nucl. Phys. B **153**, 334 (1979).
 - [3] R. N. Mohapatra and G. Senjanovic, Phys. Rev. Lett. **44**, 912 (1980).
 - [4] J. F. Gunion, J. Grifols, A. Mendez, B. Kayser and F. I. Olness, Phys. Rev. D **40**, 1546 (1989);

- J. A. Grifols, Phys. Rev. D **18**, 2704 (1978); J. A. Grifols, A. Mendez and G. A. Schuler, Mod. Phys. Lett. A **4**, 1485 (1989); N. G. Deshpande, J. F. Gunion, B. Kayser and F. I. Olness, Phys. Rev. D **44**, 837 (1991); M. L. Swartz, Phys. Rev. D **40**, 1521 (1989); R. Vega and D. A. Dicus, Nucl. Phys. B **329**, 533 (1990); K. Huitu, J. Maalampi, A. Pietila and M. Raidal, Nucl. Phys. B **487**, 27 (1997); A. Datta and A. Raychaudhuri, Phys. Rev. D **62**, 055002 (2000); G. Barenboim, M. Gorbahn, U. Nierste and M. Raidal, Phys. Rev. D **65**, 095003 (2002); K. Kiers, M. Assis and A. A. Petrov, Phys. Rev. D **71**, 115015 (2005); A. G. Akeroyd and M. Aoki, Phys. Rev. D **72**, 035011 (2005).
- [5] V. M. Abazov *et al.* [D0 Collaboration], Phys. Rev. Lett. **93**, 141801 (2004); D. E. Acosta *et al.* [CDF Collaboration], Phys. Rev. Lett. **93**, 221802 (2004); D. E. Acosta *et al.* [CDF Collaboration], Phys. Rev. Lett. **95**, 071801 (2005).
- [6] K. Agashe, A. Delgado, M. J. May and R. Sundrum, JHEP 0308, 050 (2003); K. Agashe *et al.*, Phys. Rev. D **76**, 115015 (2007); K. Agashe, S. Gopalakrishna, T. Han, G. Y. Huang and A. Soni, arXiv:0810.1497 [hep-ph].
- [7] T. Appelquist, H. C. Cheng and B. A. Dobrescu, Phys. Rev. D **64**, 035002 (2001); H. C. Cheng, K. T. Matchev and M. Schmaltz, Phys. Rev. D **66**, 056006 (2002).
- [8] N. Arkani-Hamed, A. G. Cohen, E. Katz and A. E. Nelson, JHEP 0207, 034 (2002); D. E. Kaplan and M. Schmaltz, JHEP 0310, 039 (2003); T. Han, H. E. Logan, B. McElrath and L. T. Wang, Phys. Rev. D **67**, 095004 (2003).
- [9] C. Csaki, C. Grojean, L. Pilo and J. Terning, Phys. Rev. Lett. **92**, 101802 (2004); R. S. Chivukula, B. Coleppa, S. Di Chiara, E. H. Simmons, H. J. He, M. Kurachi and M. Tanabashi, Phys. Rev. D **74**, 075011 (2006); H. J. He *et al.*, Phys. Rev. D **78**, 031701 (2008).
- [10] T. G. Rizzo, Phys. Rev. D **50** (1994) 325.
- [11] S. Gopalakrishna, T. Han, I. Lewis, Z. g. Si and Y. F. Zhou, arXiv:1008.3508 [hep-ph]; T. G. Rizzo, JHEP **0705**, 037 (2007).
- [12] P. Langacker and S. Uma Sankar, Phys. Rev. D **40**, 1569 (1989).
- [13] C. Amsler *et al.* [Particle Data Group], Phys. Lett. B **667** (2008) 1.
- [14] T. M. P. Tait and C. P. P. Yuan, Phys. Rev. D **63**, 014018 (2001); Q. H. Cao, J. Wudka and C. P. Yuan, Phys. Lett. B **658**, 50 (2007).
- [15] V. M. Abazov *et al.* [D0 Collaboration], Phys. Rev. Lett. **100**, 031804 (2008); T. Aaltonen *et al.* [The CDF Collaboration], CDF Note 9246 (2008); V. M. Abazov *et al.* [D0 Collaboration],

- Phys. Rev. Lett. **100**, 211803 (2008).
- [16] M. Frank, A. Hayreter and I. Turan, Phys. Rev. D **82**, 033012 (2010) [arXiv:1005.3074 [hep-ph]].
- [17] G. Senjanovic, Nucl. Phys. B **153**, 334 (1979); M. A. B. Beg, R. V. Budny, R. N. Mohapatra and A. Sirlin, Phys. Rev. Lett. **38**, 1252 (1977) [Erratum-ibid. **39**, 54 (1977)].
- [18] H. Harari and M. Leurer, Nucl. Phys. B **233**, 221 (1984).
- [19] K. Kiers, J. Kolb, J. Lee, A. Soni and G. H. Wu, Phys. Rev. D **66**, 095002 (2002) [arXiv:hep-ph/0205082].
- [20] P. Langacker, Phys. Rev. D **30**, 2008 (1984).
- [21] W. Ma, X. Li and Y. Liu, Phys. Rev. D **45** (1992) 1792; J. Maalampi, A. Pietila and J. Vuori, Nucl. Phys. B **381**, 544 (1992); P. Langacker, R. W. Robinett and J. L. Rosner, Phys. Rev. D **30**, 1470 (1984).
- [22] G. Barenboim, J. Bernabeu, J. Prades and M. Raidal, Phys. Rev. D **55**, 4213 (1997).
- [23] W. S. Hou and A. Soni, Phys. Rev. D **32**, 163 (1985); L. Maharana, Phys. Lett. B **149**, 399 (1984); J. M. Frere, J. Galand, A. Le Yaouanc, L. Oliver, O. Pene and J. C. Raynal, Phys. Rev. D **46**, 337 (1992); D. Chang, J. Basecq, L. F. Li and P. B. Pal, Phys. Rev. D **30**, 1601 (1984); G. Beall, M. Bander and A. Soni, Phys. Rev. Lett. **48**, 848 (1982); R. N. Mohapatra, G. Senjanovic and M. D. Tran, Phys. Rev. D **28**, 546 (1983); P. Colangelo and G. Nardulli, Phys. Lett. B **253**, 154 (1991).
- [24] A. Maiezza, M. Nemevsek, F. Nesti and G. Senjanovic, arXiv:1005.5160 [hep-ph].
- [25] F. J. Gilman and M. H. Reno, "Restrictions From The Neutral K And B Meson Systems On Left-Right Symmetric Phys. Rev. D **29**, 937 (1984); L. Maharana, A. Nath and A. R. Panda, Phys. Rev. D **47** (1993) 4998.
- [26] D. Silverman and H. Yao, JHEP **0110**, 008 (2001).
- [27] T. G. Rizzo, Phys. Rev. D **50**, 3303 (1994); G. Bhattacharyya and A. Raychaudhuri, Phys. Lett. B **357**, 119 (1995); C. S. Kim and Y. G. Kim, Phys. Rev. D **61**, 054008 (2000).
- [28] G. Beall and A. Soni, Phys. Rev. Lett. **47**, 552 (1981); J. M. Frere, J. Galand, A. Le Yaouanc, L. Oliver, O. Pene and J. C. Raynal, Phys. Rev. D **45**, 259 (1992); M. E. Pospelov, Phys. Rev. D **56**, 259 (1997).
- [29] T. Aaltonen *et. al* [CDF Collaboration], Phys. Rev. D **79**, 112002 (2009).
- [30] A. Pukhov, arXiv:hep-ph/0412191.